Electronic Supplementary Material (ESI) for Dalton Transactions.

Electronic supporting information for

Field-Induced SIM Behaviour in Early Lanthanide(III) Organophosphates Incorporating 18-crown-6

Aditya Borah, Sourav Dey, Sandeep K. Gupta, Gopalan Rajaraman and Ramaswamy Murugavel*

Infrared spectroscopy of 1-5: The FTIR spectra of all the five compounds were recorded as KBr diluted disks (Figure S1). The broad absorption peaks centred at around 2300 cm^{-1} is due to the presence of free P-OH group present in the molecular structures. The strong absorption peaks that appear in the region of 1200-1150 cm^{-1} and 1000-850 cm^{-1} are due to the presence of P=O stretching and M-O=P and M-O-P symmetric and asymmetric vibrations respectively. The broad peaks near the region of 3500 cm^{-1} are originating from the water molecules. Peaks around 2950 and 2870 cm^{-1} are due to symmetric and asymmetric vibration of the C-H bond present in the organic part of the ligand.

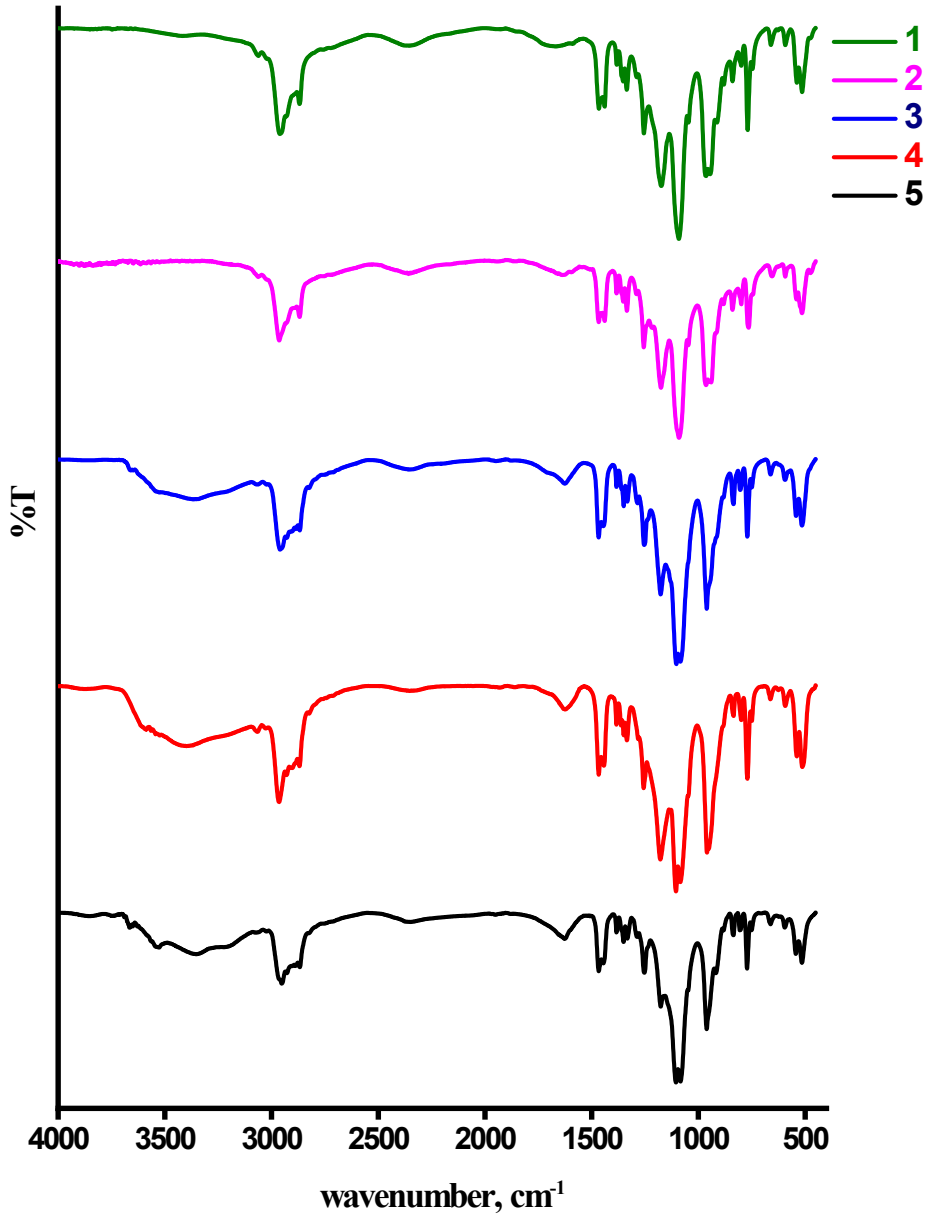

Figure S1. FTIR spectra of **1-5** (as disc diluted in KBr)

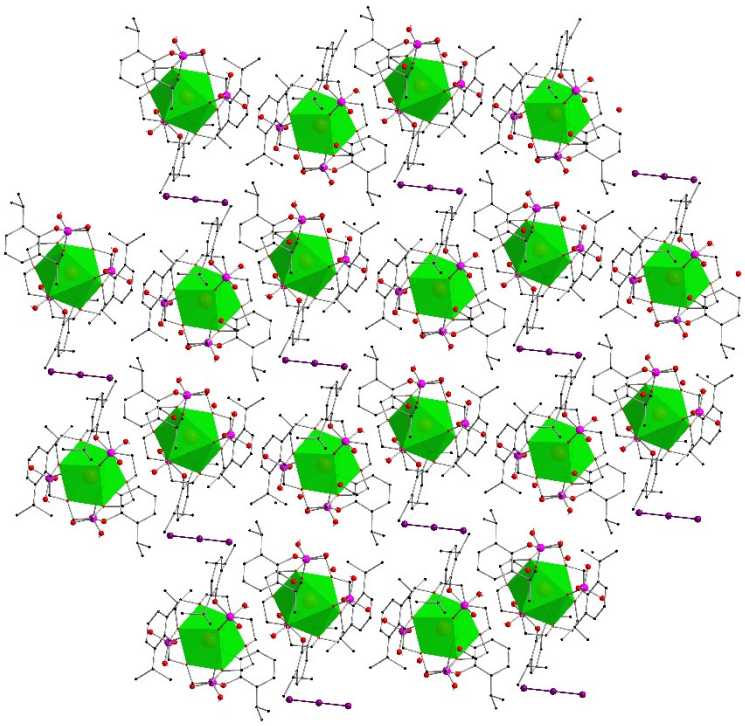

Figure S2. Lattice arrangement of **1**. H atoms are omitted for clarity, disordered I_3 ions with largest occupancy is shown here. Colour code: Ce, orange; P, pink; O, red; black, carbon and I, violet. Due to the bulkiness in the phenyl rings and lattice triiodide anions and solvent molecules, Ce centres are separated by at least 10.097 Å.

Table S1: Selected bond lengths (Å) and bond angles (°) in **1.**

Ce1-O1	2.422(5)	O2-Ce1-O6	88.94(7)	O4-Ce1-O7	151.07(8)
Ce1-O2	2.399(5)	O2-Ce1-O7	72.16(7)	O6-Ce1-O5	60.25(8)
Ce1-O3	2.330(5)	O2-Ce1-O8	71.66(8)	O6-Ce1-O7	60.13(9)
Ce1-O4	2.631(5)	O2-Ce1-O9	88.94(9)	O6-Ce1-O5	60.25(8)
Ce1-O5	2.693(5)	O3-Ce1-O1	141.74(8)	O6-Ce1-O7	60.13(9)
Ce1-O6	2.661(6)	O3-Ce1-O2	141.65(8)	O6-Ce1-O8	120.85(9)
Ce1-O7	2.670(5)	O3-Ce1-O4	76.63(9)	O7-Ce1-O5	112.65(8)
Ce1-O8	2.668(6)	O3-Ce1-O5	77.65(9)	O8-Ce1-O5	153.55(9)
Ce1-O9	2.607(6)	O3-Ce1-O6	90.50(2)	O8-Ce1-O7	60.76(9)
O1-Ce1-O4	70.25(8)	O3-Ce1-O7	74.46(8)	O9-Ce1-O4	60.40(2)
O1-Ce1-O5	69.77(6)	O3-Ce1-O8	75.90(2)	O6-Ce1-O8	120.85(9)
O1-Ce1-O6	90.36(8)	O3-Ce1-O9	91.80(2)	O7-Ce1-O5	112.65(8)
O1-Ce1-O7	136.62(8)	O4-Ce1-O5	60.57(9)	O9-Ce1-O6	177.68(9)
O1-Ce1-O8	134.05(8)	O4-Ce1-O6	120.80(9)	O9-Ce1-O7	120.0(2)
O1-Ce1-O9	88.3(2)	O4-Ce1-O7	151.08(8)	O9-Ce1-O8	59.2(2)
O2-Ce1-O1	76.64(6)	O4-Ce1-O8	111.50(2)	O9-Ce1-O5	120.9(2)
O2-Ce1-O4	134.57(7)	O4-Ce1-O6	120.80(9)		
O2-Ce1-O5	133.10(8)	O4-Ce1-O8	111.50(2)		

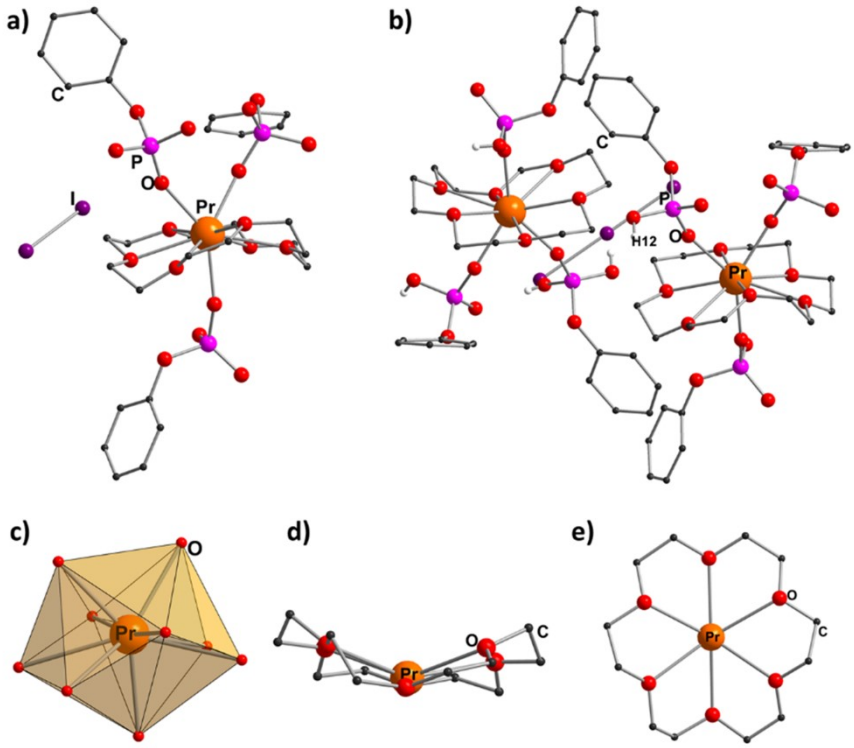

Figure S3. Molecular structure of **2**. (a) The asymmetric unit and (b) full molecule of **2**. (c) Muffin shaped coordination polyhedra around the nine-coordinated Pr(III) ion. (d) The side view and (e) top view of the binding mode of 18-crown-6 to Ce(III) centre, coordinates in a wavy fashion. The isopropyl groups on the phenyl ring, lattice solvent molecules and the hydrogen atoms (except H12 present in the spatial position) are omitted for clarity.

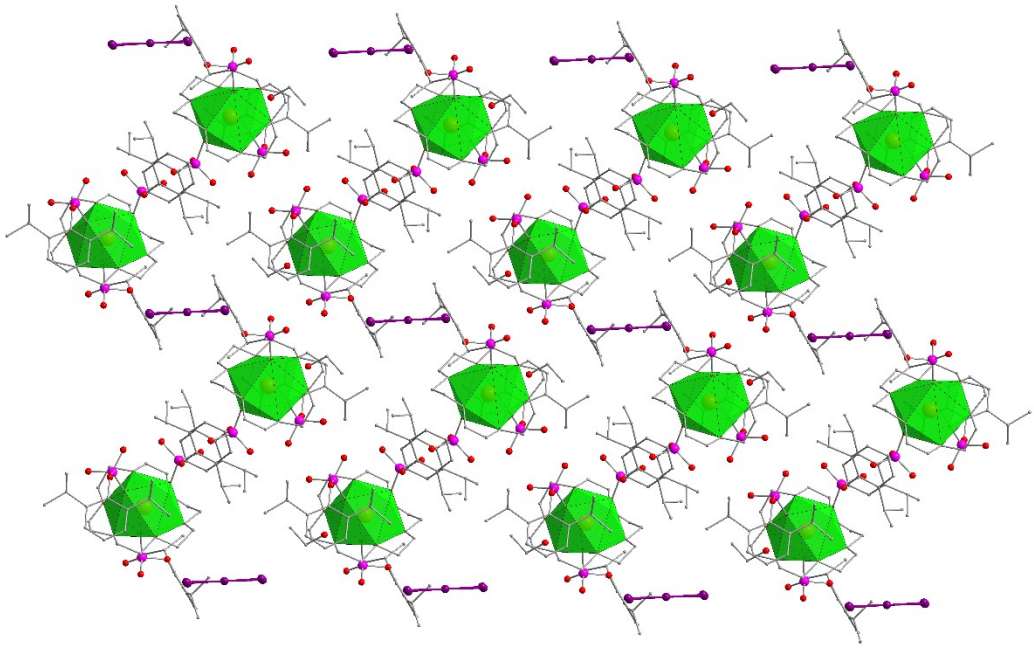

Figure S4. Lattice arrangement of **2**. H atoms are omitted for clarity. Colour code: Pr, orange; P, pink; O, red; black, carbon and I, violet. Due to the bulkiness in the phenyl rings of

organophosphates and lattice triiodide anions and lattice solvent molecules, Pr(III) centres are separated by at least 9.83 Å.

Table S2: Selected bond lengths (Å) and bond angles (°) in **2**

Pr1-O1	2.649(2)	O4-Pr1-O3	61.07(8)	O7-Pr1-O15	141.69(8)
Pr1-O2	2.608(3)	O4-Pr1-O5	60.86(8)	O11-Pr1-O1	69.33(8)
Pr1-O3	2.627(3)	O5-Pr1-O1	114.07(8)	O11-Pr1-O2	75.03(10)
Pr1-O4	2.620(2)	O6-Pr1-O1	61.85(8)	O11-Pr1-O3	82.59(9)
Pr1-O5	2.645(2)	O6-Pr1-O2	123.39(9)	O11-Pr1-O4	134.87(8)
Pr1-O6	2.584(2)	O6-Pr1-O3	169.74(9)	O11-Pr1-O5	138.29(8)
Pr1-O7	2.315(2)	O6-Pr1-O4	122.36(8)	O11-Pr1-O6	89.50(9)
Pr1-O11	2.410(2)	O6-Pr1-O5	61.55(8)	O15-Pr1-O1	132.25(8)
Pr1-O15	2.361(2)	O7-Pr1-O1	76.48(8)	O15-Pr1-O2	138.60(9)
O2-Pr1-O3	60.80(1)	O7-Pr1-O2	73.10(9)	O15-Pr1-O3	86.03(9)
O2-Pr1-O4	105.28(1)	O7-Pr1-O3	100.22(9)	O15-Pr1-O4	74.96(8)
O2-Pr1-O5	145.33(9)	O7-Pr1-O4	75.38(8)	O15-Pr1-O5	72.00(8)
O3-Pr1-O1	120.54(9)	O7-Pr1-O5	72.60(8)	O15-Pr1-O6	85.79(8)
O3-Pr1-O5	121.34(8)	O7-Pr1-O6	90.04(8)	O15-Pr1-O11	76.83(8)
O4-Pr1-O1	151.51(8)	O7-Pr1-O11	141.28(8)		

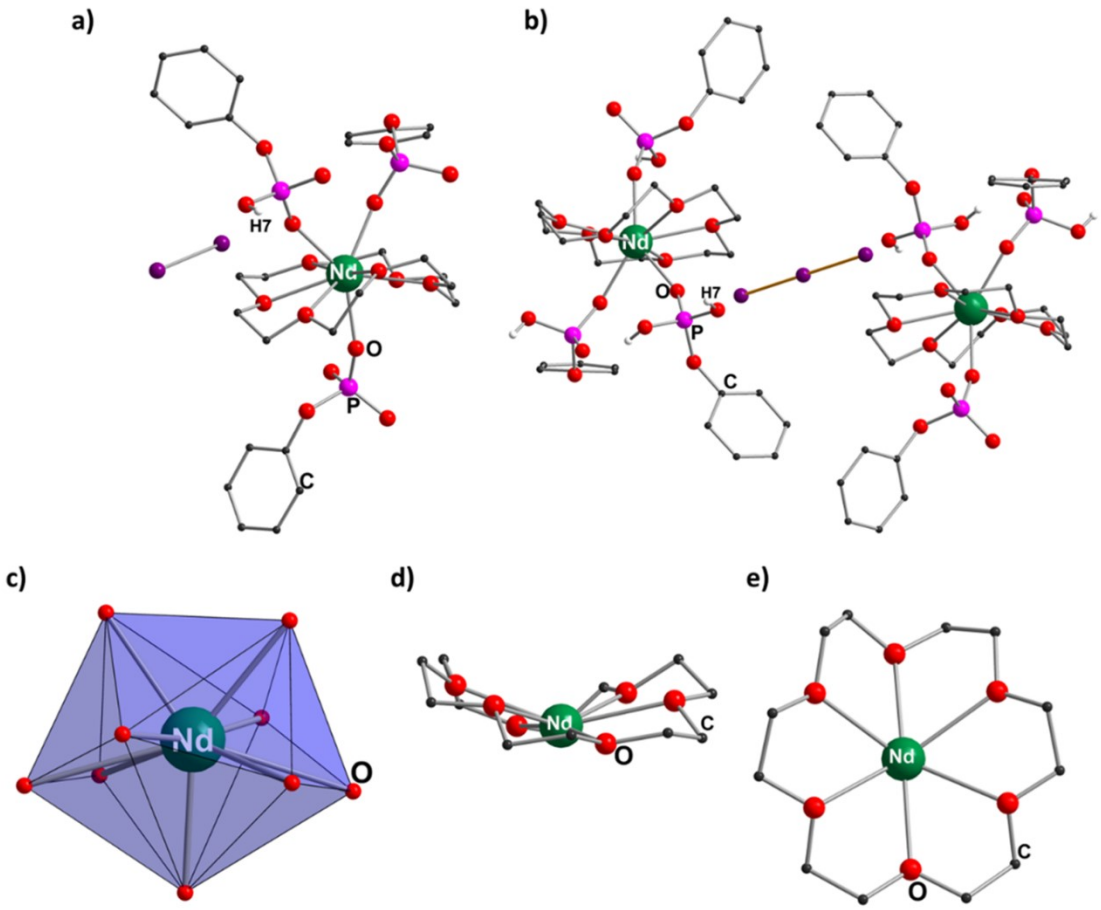

Figure S5. Molecular structure of **3**. (a) The asymmetric unit and (b) full molecule of **3**. (c) Muffin shaped coordination polyhedra around the nine-coordinated Nd(III) ion. (d) The side view and (e) top view of the binding mode of 18-crown-6 to Nd(III) centre, coordinates in a wavy fashion. The isopropyl groups on the phenyl ring, lattice solvent molecules and the hydrogen atoms (except H7 present in the spatial position) are omitted for clarity.

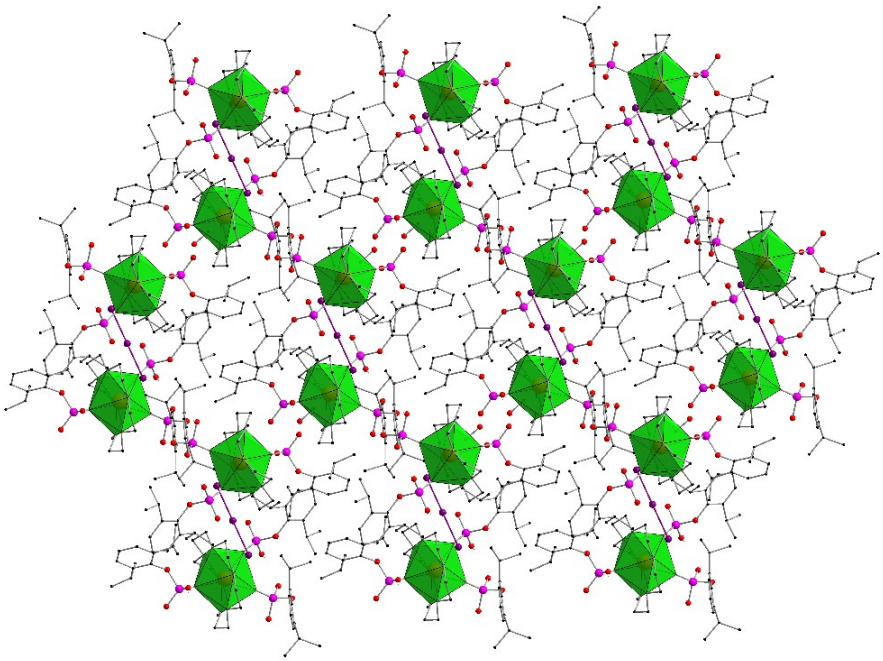

Figure S6. Lattice arrangement of **3**. H atoms are omitted for clarity. Colour code: Nd, orange; P, pink; O, red; black, carbon and I, violet. Due to the bulkiness in the phenyl rings of organophosphates and lattice triiodide anions and lattice solvent molecules, Nd(III) centres are separated by at least 9.86 Å.

Table S3: Selected bond lengths (Å) and bond angles (°) in **3.**

Nd1-O1	2.317(4)	O9-Nd1-O13	72.08(5)	O9-Nd1-O5	76.08(6)
Nd1-O5	2.387(4)	O9-Nd1-O14	75.47(7)	O15-Nd1-O17	120.57(6)
Nd1-O9	2.351(4)	O9-Nd1-O15	89.46(7)	O16-Nd1-O13	146.99(4)
Nd1-O13	2.656(5)	O9-Nd1-O16	138.29(5)	O16-Nd1-O14	107.80(6)
Nd1-O14	2.623(5)	O9-Nd1-O17	129.47(6)	O16-Nd1-O17	61.28(5)
Nd1-O15	2.577(5)	O9-Nd1-O18	82.80(5)	O17-Nd1-O13	113.90(4)
Nd1-O16	2.588(5)	O14-Nd1-O13	60.78(5)	O18-Nd1-O13	61.32(5)
Nd1-O17	2.628(5)	O14-Nd1-O17	153.58(5)	O18-Nd1-O14	121.86(5)
Nd1-O18	2.575(5)	O15-Nd1-O13	120.84(6)	O18-Nd1-O15	170.82(5)
O5-Nd1-O17	70.04(5)	O15-Nd1-O14	60.24(6)	O18-Nd1-O16	123.39(5)
O5-Nd1-O18	91.33(5)	O15-Nd1-O16	60.47(6)	O18-Nd1-O17	62.16(4)

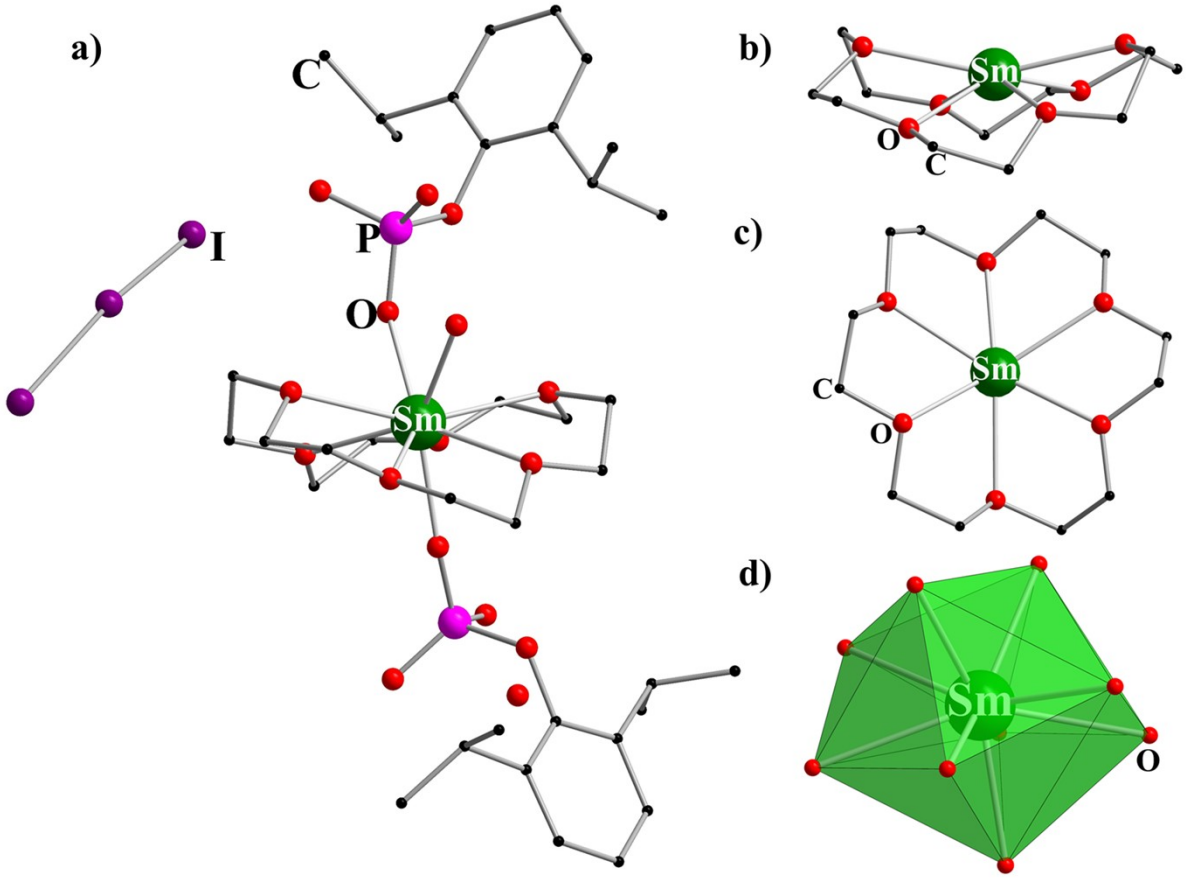

Figure S7. (a) Molecular structure of [{Sm(18-crown-6)(dippH)$_2$(H$_2$O)}·{I$_3$}] (**4**). The hydrogen atoms are omitted for clarity. (b) The side view and (c) the top view of the binding mode of 18-crown-6 to the Sm(III) centre, coordinates in a wavy fashion. (d) The coordination environment of nine-coordinated Sm(III) ion with Muffin shaped geometry.

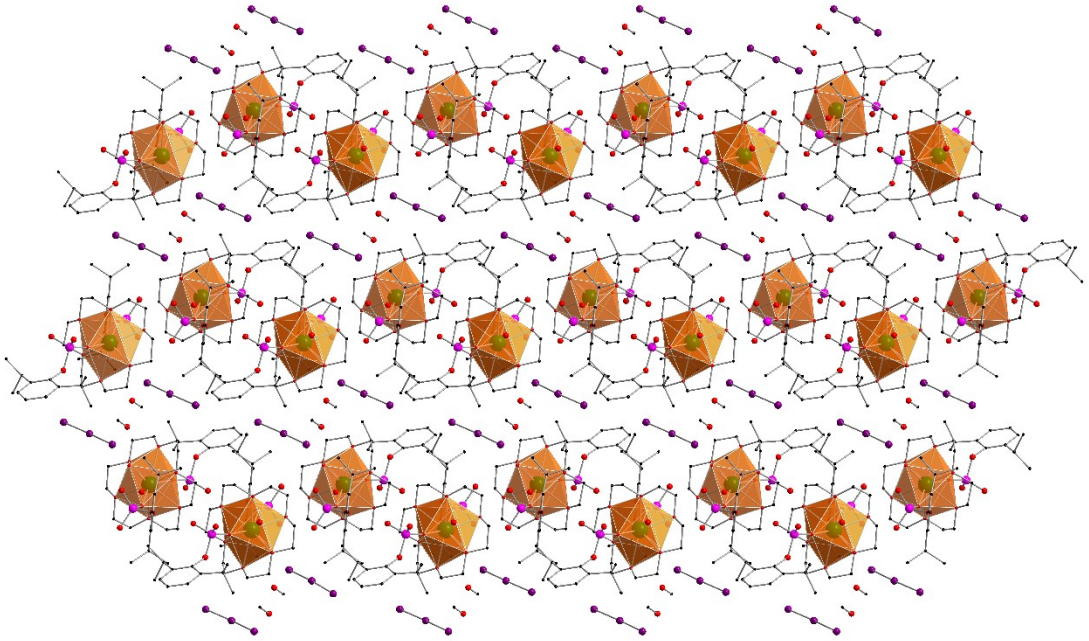

Figure S8. Lattice arrangement of **4**. H atoms are omitted for clarity. Colour code: Sm, dark blue; P, pink; O, red; black, carbon and I, violet. Due to the bulkiness in the phenyl rings of organophosphates and lattice triiodide anions and lattice solvent molecules, Sm(III) centres are separated by at least 10.12 Å.

Table S4: Selected bond lengths (Å) and bond angles (°) in **4**

Sm1-O1	2.294(3)	O1-Sm1-O15	133.02(1)	O10-Sm1-O15	62.06(10)
Sm1-O5	2.277(3)	O5-Sm1-O1	142.24(1)	O11-Sm1-O10	63.08(10)
Sm1-O9	2.403(3)	O5-Sm1-O9	140.37(1)	O11-Sm1-O13	122.75(10)
Sm1-O10	2.574(3)	O5-Sm1-O10	79.14(11	O11-Sm1-O14	155.37(11)
Sm1-O11	2.554(3)	O5-Sm1-O11	114.52(11)	O11-Sm1-O15	121.43(10)
Sm1-O12	2.504(3)	O5-Sm1-O12	79.04(11)	O12-Sm1-O10	104.02(11)
Sm1-O13	2.572(3)	O5-Sm1-O13	71.64(11)	O12-Sm1-O11	62.88(10)
Sm1-O14	2.558(3)	O5-Sm1-O14	90.11(11)	O12-Sm1-O13	63.15(10)
Sm1-O15	2.603(3)	O5-Sm1-O15	73.11(10)	O12-Sm1-O14	126.24(10)
O1-Sm1-O9	74.59(1)	O9-Sm1-O10	76.57(11)	O12-Sm1-O15	150.65(10)
O1-Sm1-O10	134.14(1)	O9-Sm1-O11	81.10(11)	O13-Sm1-O10	149.71(10)
O1-Sm1-O11	77.75(1)	O9-Sm1-O12	137.22(11)	O13-Sm1-O15	114.78(10)
O1-Sm1-O12	75.78(1)	O9-Sm1-O13	132.19(11)	O14-Sm1-O10	125.51(10)
O1-Sm1-O13	72.03(1)	O9-Sm1-O14	79.33(11)	O14-Sm1-O13	63.44(10)
O1-Sm1-O14	82.72(1)	O9-Sm1-O15	67.94(11)	O14-Sm1-O15	63.68(10)

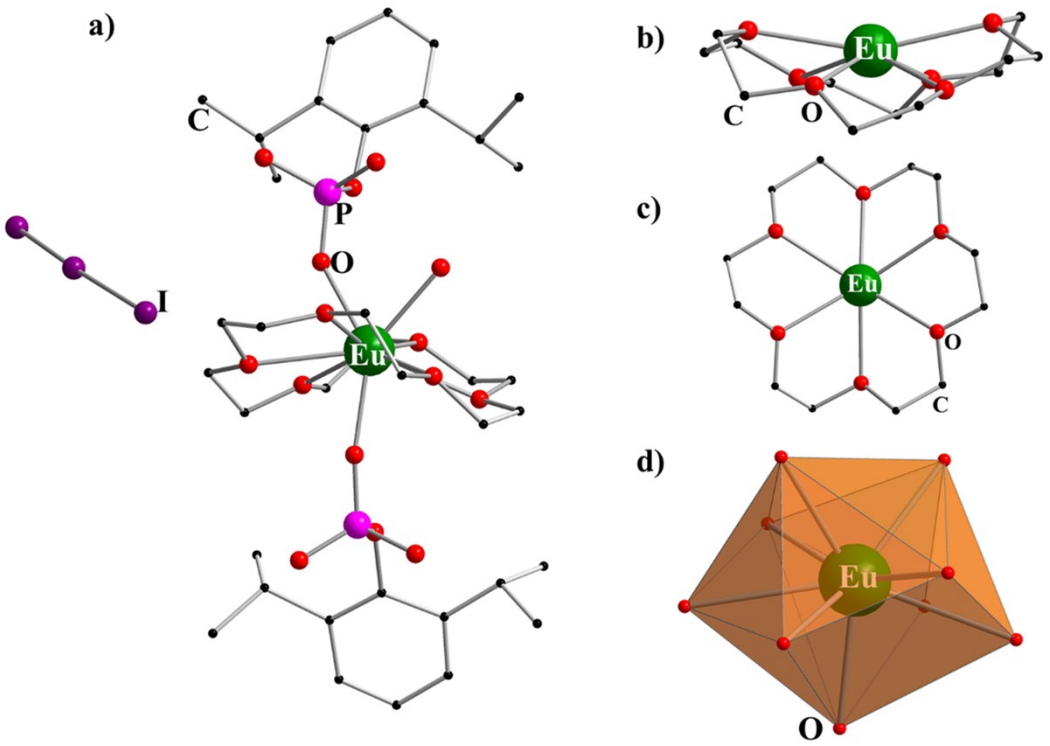

Figure S9. (a) Molecular structure of [{Eu(18-crown-6)(dippH)$_2$(H$_2$O)}·{I$_3$}] (**5**) (Only one of the two **5** present in the asymmetric unit is shown). The hydrogen atoms are omitted for clarity. (b) The side view and (c) the top view of the binding mode of 18-crown-6 to the Eu(III) centre, coordinates in a wavy fashion. (d) The coordination environment of nine-coordinated Eu(III) ion with Muffin shaped geometry.

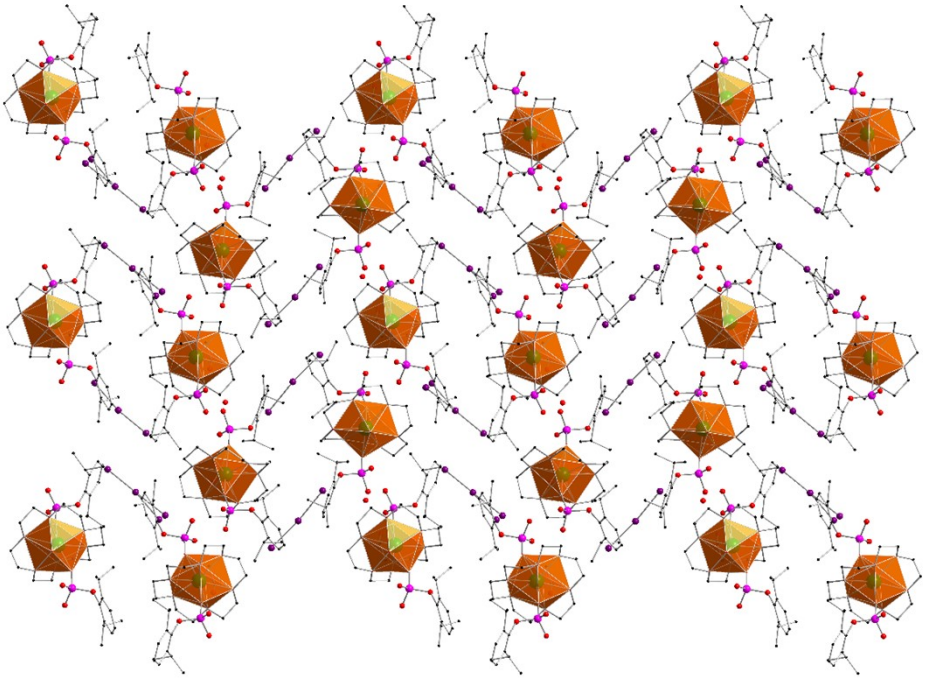

Figure S10. Lattice arrangement of **5**. H atoms are omitted for clarity. Colour code: Eu, dark blue; P, pink; O, red; black, carbon and I, violet. Due to the bulkiness in the phenyl rings of

organophosphates and lattice triiodide anions and lattice solvent molecules, Eu(III) centres are separated by at least 10.84 Å.

Table S5: Selected bond lengths (Å) and bond angles (°) in **5.**

Eu1-O1	2.587(1)	O6- Eu1-O13	76.0(4)	O16- Eu2-O26	73.5(3)
Eu1-O5	2.366(1)	O6- Eu1-O14	78.2(4)	O20- Eu2-O21	82.3(4)
Eu1-O6	2.227(9)	O6- Eu1-O15	76.1(4)	O20-Eu2-O22	74.7(4)
Eu1-O10	2.285(9)	O10- Eu1-O1	71.3(4)	O20-Eu2-O23	69.7(3)
Eu1-O11	2.566(9)	O10- Eu1-O5	74.8(4)	O20-Eu2-O24	80.4(3)
Eu1-O12	2.493(2)	O10- Eu1-O11	70.4(3)	O20-Eu2-O25	133.3(3)
Eu1-O13	2.569(1)	O10- Eu1-O12	87.1(4)	O20-Eu2-O26	136.3(3)
Eu1-O14	2.597(2)	O10- Eu1-O13	136.0(4)	O21-Eu2-O22	63.2(3)
Eu1-O15	2.556(2)	O10- Eu1-O14	129.5(4)	O21-Eu2-O23	122.7(3)
Eu2-O16	2.283(9)	O10- Eu1-O15	75.5(4)	O21-Eu2-O25	123.0(3)
Eu2-O20	2.373(9)	O11- Eu1-O1	117.7(4)	O21-Eu2-O26	62.4(3)
Eu2-O21	2.532(9)	O11- Eu1-O13	122.1(4)	O22-Eu2-O25	149.8(3)
Eu2-O22	2.582(9)	O11- Eu1-O14	150.6(4)	O23-Eu2-O22	61.7(3)
Eu2-O23	2.577(9)	O12- Eu1-O1	153.9(4)	O23-Eu2-O25	112.2(3)
Eu2-O24	2.521(9)	O12- Eu1-O11	65.7(4)	O24-Eu2-O21	157.9(3)
Eu2-O25	2.612(9)	O12- Eu1-O13	66.5(4)	O24-Eu2-O22	124.3(3)
Eu2-O26	2.570(9)	O12- Eu1-O14	128.4(4)	O24-Eu2-O23	63.0(3)
Eu2-O27	2.261(9)	O12- Eu1-O15	129.3(5)	O24-Eu2-O25	62.8(3)
O1- Eu1-O14	62.7(4)	O13- Eu1-O1	119.8(4)	O24-Eu2-O26	124.6(3)
O5- Eu1-O1	81.5(5)	O13- Eu1-O14	62.0(4)	O26-Eu2-O22	107.4(4)
O5- Eu1-O11	130.6(5)	O15- Eu1-O1	60.3(5)	O26-Eu2-O23	151.0(3)
O5- Eu1-O12	78.7(5)	O15- Eu1-O11	63.6(5)	O26-Eu2-O25	62.5(3)
O5- Eu1-O13	66.2(4)	O15- Eu1-O13	148.4(4)	O27-Eu2-O16	142.6(3)
O5- Eu1-O14	78.7(4)	O15- Eu1-O14	97.8(4)	O27-Eu2-O20	142.0(3)
O5- Eu1-O15	137.3(4)	O16- Eu2-O20	75.3(3)	O27-Eu2-O21	104.3(3)
O6-Eu1-O1	113.7(4)	O16- Eu2-O21	79.2(3)	O27-Eu2-O22	75.4(3)
O6-Eu1-O5	141.7(3)	O16- Eu2-O22	134.2(3)	O27-Eu2-O23	75.7(3)
O6-Eu1-O10	142.6(3)	O16- Eu2-O23	134.3(3)	O27-Eu2-O24	97.8(3)
O6- Eu1-O11	75.3(3)	O16- Eu2-O24	83.2(3)	O27-Eu2-O25	74.5(3)
O6- Eu1-O12	92.4(4)	O16- Eu2-O25	72.8(3)	O27-Eu2-O26	75.5(3)

Table S6: Crystal Data and Structure Refinement Details for **1-5**

Identification code	**1**	**2**	**3**	**4**	**5**
Empirical formula	$C_{98}H_{155}Ce_2I_3O_{38}P_6$	$C_{100}H_{163}I_3O_{38}P_6Pr_2$	$C_{97}H_{160}I_3Nd_2O_{37}P_6$	$C_{37}H_{68}I_{2.38}O_{17}P_2Sm$	$C_{37}H_{62}EuI_3O_{17}P_2$
Formula weight	2787.97	2821.63	2773.24	1298.59	1373.46
Temperature/K	150.0	150.0	150.0	150.0	150.0
Crystal system	Triclinic	Triclinic	Triclinic	Triclinic	Triclinic
Space group	$P\bar{1}$	$P\bar{1}$	$P\bar{1}$	$P\bar{1}$	$P\bar{1}$
a/Å	14.6386(3)	14.3319(2)	14.3480(8)	13.0040(8)	12.5932(6)
b/Å	15.8305(5)	15.0410(2)	15.8035(9)	13.2938(6)	16.6149(5)
c/Å	16.1766(4)	17.6013(2)	17.2262(8)	15.9969(8)	25.0246(9)
α/°	108.616(2)	111.835(6)	67.693(5)	76.591(4)	89.081(3)
β/°	98.084(2)	90.642(1)	88.567(4)	84.307(5)	89.653(3)
γ/°	106.682(2)	111.769(4)	63.094(6)	73.542(5)	85.828(3)
Volume/Å^3	3289.79(6)	3221.52(8)	3171.1(3)	2578.2(2)	5221.4(3)
Z	1	1	1	2	4
ρ_{calc}g/cm^3	1.407	1.454	1.452	1.673	1.747
μ/mm^{-1}	1.529	1.612	1.686	2.684	3.097
F(000)	1412.0	1434.0	1407.0	1288.0	2688.0
Crystal size/mm^3	0.15 × 0.11 × 0.1	0.2 × 0.1 × 0.06	0.2 × 0.15 × 0.15	0.15 × 0.12 × 0.1	0.15 × 0.11 × 0.1
Radiation	Mo Kα (λ = 0.71073)	Mo Kα (λ = 0.71073)	Mo Kα (λ = 0.71073)	MoKα (λ = 0.71073)	MoKα (λ = 0.71073)
2Θ range for data collection/°	4.546 to 49.994	4.808 to 50	4.494 to 50	3.27 to 54.998	3.242 to 49.998
Index ranges	-17 ≤ h ≤ 17, -18 ≤ k ≤ 18, -19 ≤ l ≤ 19	-17 ≤ h ≤ 17, -17 ≤ k ≤ 17, -20 ≤ l ≤ 20	-17 ≤ h ≤ 17, -18 ≤ k ≤ 18, -20 ≤ l ≤ 20	-16 ≤ h ≤ 16, -16 ≤ k ≤ 17, -20 ≤ l ≤ 20	-14 ≤ h ≤ 14, -19 ≤ k ≤ 19, -29 ≤ l ≤ 29
Reflections collected	100090	121284	121941	66179	90519
Independent reflections	11568 [R_{int} = 0.0954, R_{sigma} = 0.0556]	11252 [R_{int} = 0.0456, R_{sigma} = 0.0184]	11155 [R_{int} = 0.1030, R_{sigma} = 0.0489]	11757 [R_{int} = 0.0559, R_{sigma} = 0.0420]	18292 [R_{int} = 0.1362, R_{sigma} = 0.1214]
Data/restraints/parameters	11568/7/707	11252/0/703	11155/0/699	11757/0/593	18292/38/1127
Goodness-of-fit on F^2	1.064	1.045	1.026	1.146	1.077
Final R indexes [I>=2σ (I)]	R_1 = 0.0866, wR_2 = 0.2264	R_1 = 0.0353, wR_2 = 0.0896	R_1 = 0.0618, wR_2 = 0.1588	R_1 = 0.0446, wR_2 = 0.1035	R_1 = 0.1008, wR_2 = 0.2028
Final R indexes [all data]	R_1 = 0.1013, wR_2 = 0.2411	R_1 = 0.0368, wR_2 = 0.0911	R_1 = 0.0817, wR_2 = 0.1828	R_1 = 0.0528, wR_2 = 0.1150	R_1 = 0.1557, wR_2 = 0.2410
Largest diff. peak/hole / e Å^{-3}	1.82/-1.14	1.84/-0.90	2.00/-2.27	2.77/-1.56	2.94/-1.07

Table S7: Ln-Ln distances in **1-5.**

Complex	**Minimum Ln-Ln distances (Å)**
1	10.096
2	9.83
3	10.79
4	10.12
5	9.69

***SHAPE analysis of* 1-5.** The coordination environment of nine coordinated Ln(III) ions in **1-5** were analysed by SHAPE 2.1 software[1]. Continuous Shape measurements show that the [LnO_9] cores in all the complexes, **1-5**, have the same geometry around the respective Ln(III) centres with minimal deviation from ideal *C*s symmetry, indicating a muffin geometry around it.

Table S8: Continuous SHAPE measurements[1] of the coordination polyhedra of Ln(III) ion of type LnO_9 for **1-5**.

Structure [ML9]	Symmetry	**1**	**2**	**3**	**4**	**5**
EP-9	D9h	32.161	32.066	31.959	31.858	32.493
OPY-9	C8v	20.66	20.673	21.131	21.190	21.336
HBPY-9	D7h	14.976	14.763	15.840	16.086	16.400
JTC-9	C3v	15.278	15.315	13.088	13.018	13.698
JCCU-9	C4v	6.936	7.139	8.142	8.330	7.313
CCU-9	C4v	6.003	6.224	7.051	7.282	6.310
JCSAPR-9	C4v	5.658	5.552	4.050	3.671	3.613
CSAPR-9	C4v	4.453	4.388	3.045	2.738	2.743
JTCTPR-9	D3h	5.126	4.981	3.703	3.284	2.982
TCTPR-9	D3h	5.520	5.421	3.969	3.600	3.190
JTDIC-9	C3v	11.968	12.068	11.333	11.628	11.747
HH-9	C2v	4.448	4.473	5.213	5.703	5.706
MFF-9	**Cs**	**3.160**	**3.189**	**2.334**	**2.166**	**2.349**

Label	**Shape**
EP-9	Enneagon
OPY-9	Octagonal pyramid
HBPY-9	Heptagonal bipyramid
JTC-9	Johnson triangular cupola J3
JCCU-9	Capped cube J8
CCU-9	Spherical-relaxed capped cube
JCSAPR-9	Capped square antiprism J10
CSAPR-9	Spherical capped square antiprism
JTCTPR-9	Tricapped trigonal prism J51
TCTPR-9	Spherical tricapped trigonal prism
JTDIC-9	Tridiminished icosahedron J63
HH-9	Hula-hoop
MFF-9	Muffin

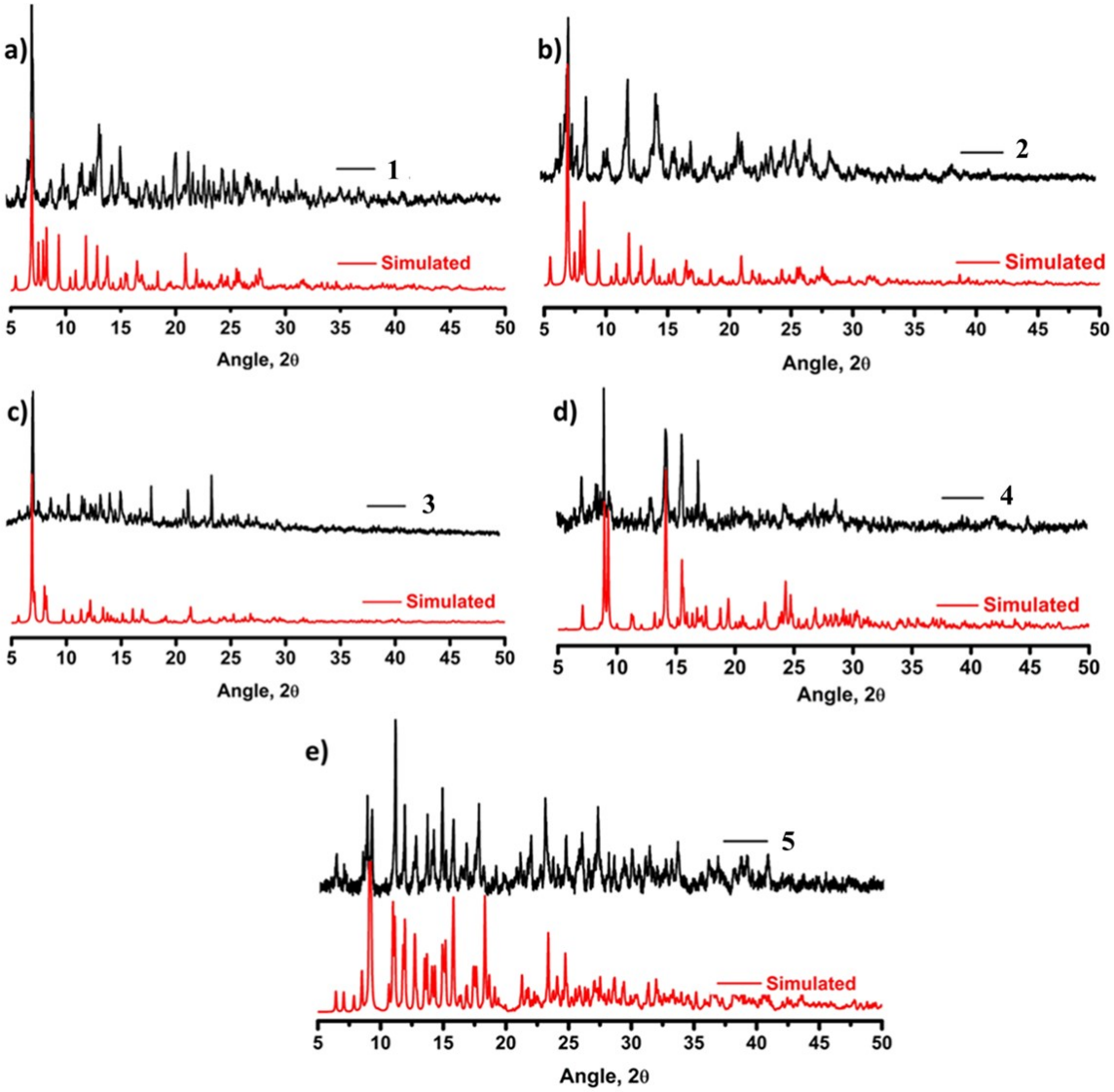

Figure S11: The simulated (red) and experimental (black) PXRD patterns of **1-5**.

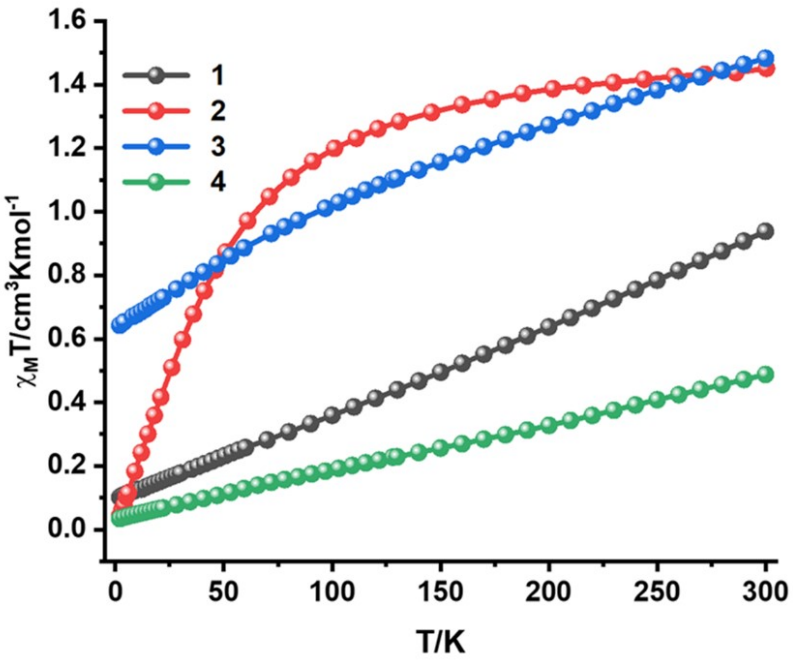

Figure S12: The temperature-dependence of magnetization data for **1**-**4** for the temperature range of 2 K to 300 K in presence of 0.1T magnetic field.

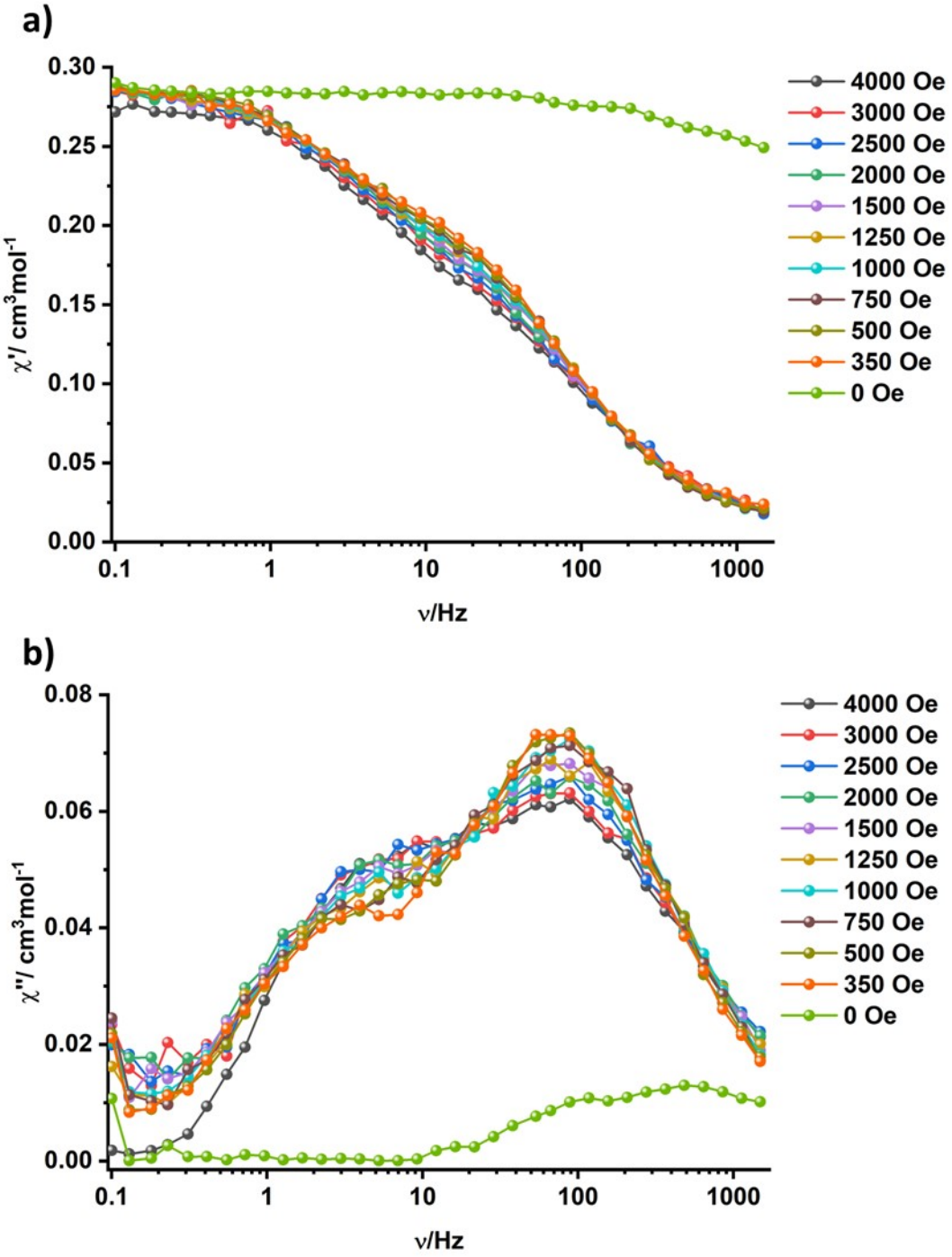

Figure S13: Frequency dependence (a) in phase and (b) out-of-phase magnetic susceptibility signals of **1** at 1.8 in the presence of different indicated external magnetic fields of range 0-4000 Oe.

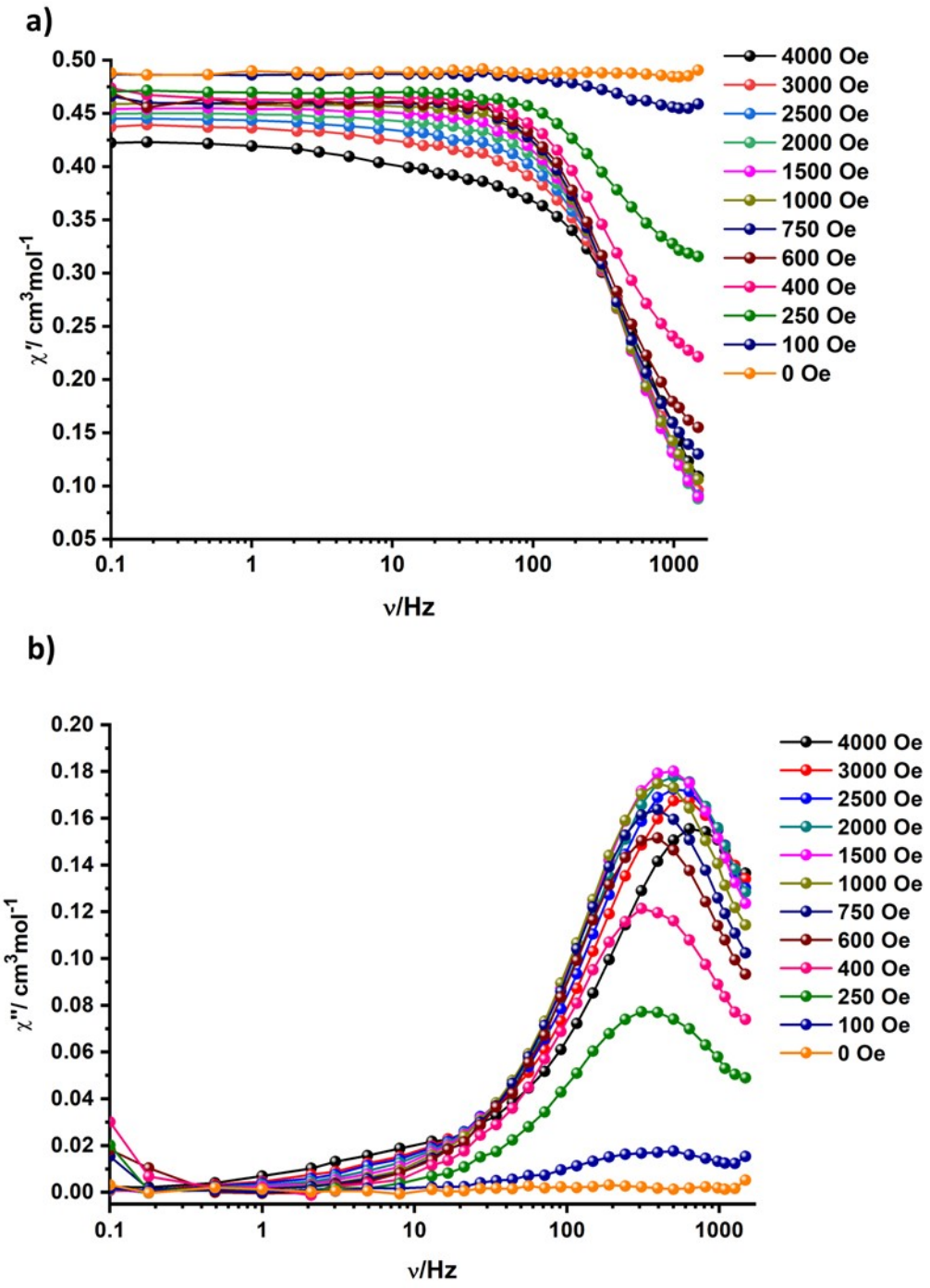

Figure S14: Frequency dependence (a) in phase and (b) out-of-phase magnetic susceptibility signals of **3** at 1.8 for in the presence of different indicated external magnetic fields of range 0-4000 Oe.

Table S9: Relaxation fitting parameters from the least-square fitting of the Cole-Cole plots of compound **1** under 350 Oe dc field according to the modified Debye model considering two relaxation processes.

T/K	τ_1	τ_1_err	Dχ_1 (cm^3/mol)	Dχ_1_err (cm^3/mol)	α_1	α_1_err	τ_2	τ_2_err	Dχ_2 (cm^3/mol)	Dχ_2_err (cm^3/mol)	α_2	α_2_err	χ_{total}	χ_{total_err}
1.8	6.94E-02	3.12E-03	8.73E-02	4.00E-03	1.75E-01	1.97E-02	2.10E-03	4.91E-05	2.25E-01	3.94E-03	2.28E-01	8.03E-03	1.76E-02	7.97E-04
2.1	4.89E-02	1.20E-03	6.79E-02	1.94E-03	1.23E-01	1.19E-02	1.46E-03	2.21E-05	2.01E-01	2.12E-03	2.57E-01	5.23E-03	1.28E-02	5.25E-04
2.4	3.30E-02	8.06E-04	5.95E-02	1.75E-03	1.17E-01	1.14E-02	9.94E-04	1.56E-05	1.77E-01	2.06E-03	2.61E-01	5.85E-03	1.09E-02	5.69E-04
2.7	2.23E-02	7.56E-04	5.21E-02	2.22E-03	1.21E-01	1.47E-02	6.73E-04	1.44E-05	1.58E-01	2.81E-03	2.71E-01	8.92E-03	9.81E-03	8.65E-04
3.0	1.25E-02	4.57E-04	5.36E-02	2.22E-03	1.57E-01	1.21E-02	4.23E-04	8.74E-06	1.34E-01	2.94E-03	2.48E-01	1.06E-02	1.00E-02	9.69E-04
3.3	8.45E-03	5.75E-04	5.36E-02	3.44E-03	1.70E-01	2.01E-02	2.82E-04	8.61E-06	1.12E-01	4.92E-03	1.87E-01	2.27E-02	1.48E-02	1.99E-03
3.6	5.74E-03	3.48E-04	4.73E-02	3.13E-03	1.57E-01	1.76E-02	1.71E-04	5.09E-06	1.12E-01	5.64E-03	2.23E-01	2.58E-02	6.07E-03	2.90E-03

Table S10: Relaxation fitting parameters from the least-square fitting of the Cole-Cole plots of compound **3** under 1.5 kOe dc field according to the generalized Debye model.

T/K	χ_s	χ_T	τ	α
1.8	0.0332	0.562	3.32E-04	0.108
2.0	0.0295	0.507	2.45E-04	0.107
2.2	0.0262	0.467	1.91E-04	0.104
2.4	0.0232	0.426	1.43E-04	0.0954
2.6	0.0223	0.394	1.10E-04	0.0846

Table S11: The computed crystal field parameters (CFP) of complexes **1** and **3** and models **1a** and **3a**. The CFPs have been computed according to the Stevens Hamiltonian;

$$\hat{H}_{CF} = \sum_{k=2,4,6} \sum_{q=-k}^{q=+k} B_k^q \tilde{O}_k^q$$

where B_k^q is the CFP and $\tilde{O}_k^q$ is the Stevens operator.

k	q	B_k^q			
		1	**1a**	**3**	**3a**
2	-2	5.51E+00	-5.95E-01	1.55E+00	3.98E-01
	-1	4.21E+01	-7.82E+01	-9.90E-01	-3.60E-01
	0	**-4.66E+01**	**-1.10E+02**	**-4.31E+00**	**-1.15E+01**
	1	6.17E+00	9.28E+00	-1.40E+00	4.87E-01
	2	-8.97E+00	1.56E+01	1.23E+00	6.48E+00
4	-4	1.52E+00	-1.49E-01	-2.12E-02	1.62E-02
	-3	2.84E+00	1.06E-01	-2.79E-01	-2.17E-01
	-2	-6.16E-01	-4.93E-01	1.71E-02	1.53E-02
	-1	-4.97E+00	1.37E+01	8.15E-02	-9.87E-02
	0	2.97E-01	1.01E-02	-2.44E-02	-3.07E-02
	1	-1.58E+00	-7.40E-01	4.83E-02	-1.00E-02
	2	-2.41E+00	2.33E-02	7.83E-02	1.36E-01
	3	-8.86E+00	1.04E+00	6.65E-02	-4.21E-02
	4	-2.64E+00	7.76E-01	-6.86E-02	-6.11E-02
6	-6			-1.65E-02	-9.12E-04
	-5			2.41E-02	1.56E-02
	-4			4.49E-03	1.79E-03
	-3			4.63E-03	-1.02E-02
	-2			-1.50E-03	1.48E-03
	-1			2.35E-03	-7.68E-03
	0			-8.72E-04	-9.17E-04
	1			-4.57E-04	-2.62E-03
	2			1.08E-03	6.63E-03
	3			1.26E-02	4.68E-04
	4			-3.26E-03	-7.14E-03
	5			-6.60E-02	5.21E-03
	6			1.21E-03	2.40E-03

Table S12: The computed LoProp charge of metal and its coordinated atoms in complexes **1** and **3**.

Complex **1**		Complex **3**	
Ce	2.5058	Nd	2.5296
O(P)	-1.1288	O(P)	-1.1346
O(P)	-1.1171	O(P)	-1.1237
O(P)	-0.7648	O(P)	-0.7693
O(Crown)	-0.5290	O(Crown)	-0.5329
O(Crown)	-0.5140	O(Crown)	-0.5167
O(Crown)	-0.5103	O(Crown)	-0.5136
O(Crown)	-0.4908	O(Crown)	-0.4934
O(Crown)	-0.4857	O(Crown)	-0.4882
O(Crown)	-0.4920	O(Crown)	-0.4945

Table S13. The CASSCF/RASSI-SO/SINGLE_ANISO calculated g tensor, m_J composition and g_{zz} angles of three ground state KDs of **1a**.

Energy (cm^{-1})	g_x	g_y	g_z	m_J composition	Angle between g_{zz} of higher KDs with KD1 (°)
0.0	0.063	0.134	4.089	1.00|±5/2>	
1128.2	0.745	1.390	2.094	0.82|±3/2>+0.18|±1/2>	7.083
2179.1	1.204	1.092	3.062	0.82|±1/2>+0.18|±3/2>	93.960

Table S14. The CASSCF/RASSI-SO/SINGLE_ANISO calculated g tensor, m_J composition and g_{zz} angles of three ground state KDs of **3a**.

Energy (cm^{-1})	g_x	g_y	g_z	m_J composition	Angle between g_{zz} of higher KDs with KD1 (°)
0.0	0.049	0.062	6.096	0.94|±9/2>+0.04|±5/2>	
449.6	0.340	0.398	4.913	0.84|±7/2>+0.09|±5/2>+0.05|±3/2>	22.587
601.8	1.185	1.492	4.266	0.71|±5/2>+0.17|±3/2>+0.07|±1/2>	53.861
680.4	0.751	1.609	3.591	0.55|±3/2>+0.15|±1/2>+0.15|±7/2>	63.542
830.3	0.335	0.851	6.076	0.75|±1/2>+0.22|±3/2>	91.254

References:

1. Llunell, M.; Casanova, D.; Cirera, J.; Alemany, P.; Alvarez, S., SHAPE, version 2.1. *Universitat de Barcelona, Barcelona, Spain* **2013,** *2103*.